

## Effects of an adjacent metal surface on spin wave propagation

Jonathan Trossman,<sup>1,a</sup> Jinho Lim,<sup>1</sup> Wonbae Bang,<sup>1</sup> J. B. Ketterson,<sup>1</sup>  
 C. C. Tsai,<sup>2</sup> and S. J. Lee<sup>3</sup>

<sup>1</sup>Physics and Astronomy, Northwestern University, Evanston, IL 60208, USA

<sup>2</sup>Chang Jung Christian University, Zhangda Rd, Guiren District, Tainan city, Taiwan, 711

<sup>3</sup>Department of Physics, Research Institute for Natural Sciences, Hanyang University, Seoul 133-791, South Korea

(Presented 7 November 2017; received 1 October 2017; accepted 15 November 2017;  
 published online 9 January 2018)

We experimentally investigate and model the effects of a copper surface adjacent to a surface on which spin waves propagate in a thin film of yttrium iron garnet (YIG). Investigation was performed using a phase detection method, which can map out the spin wave velocity as a function of wavevector for small wavevector with high resolution. This velocity is in good agreement with a simple model and allows for extraction of the separation between the YIG film and the copper. © 2018 Author(s). All article content, except where otherwise noted, is licensed under a Creative Commons Attribution (CC BY) license (<http://creativecommons.org/licenses/by/4.0/>). <https://doi.org/10.1063/1.5007253>

### I. INTRODUCTION

There is currently much interest in various effects associated with spin-orbit coupling that arise from metal layers in contact with ferromagnetic films, examples being spin pumping and interfacial Dzyaloshinskii-Moriya interactions (DMI).<sup>1</sup> When considering dynamic responses involving the propagation of the wave, one must also account for the current induced in the adjacent metal layer which, in turn, affects the propagation of the wave itself.<sup>2</sup> In free space, the amplitude of the magnetic field accompanying a spin wave decays exponentially with a characteristic length equal to  $1/k$ , where  $k$  in the wavevector of the spin wave. For the case of a perfect conductor in contact with the film, the field must vanish at the interface.

The in-plane dispersion of spin waves in an infinite slab was treated long ago by Damon and Eshbach<sup>3-6</sup> where two principal modes were identified: a surface wave, now termed the Damon-Eshbach (DE) mode, and a so called backward volume (BV) mode. Here we report measurements of the variation of the velocity with wavevector resulting from an adjacent copper film for the DE mode in an insulating ferromagnet, yttrium iron garnet (YIG).

Figure 1 shows frequency vs. wavevector for a 3.05 micron film in a field of 1.4 kG according to the Damon-Eshbach theory. The velocity in the low  $k$ , dipole dominated, regime for the DE mode is given by

$$V = \frac{4\gamma^2 s \pi^2 M^2}{\omega_0}; \quad (1)$$

where  $\gamma$  is the gyromagnetic ratio,  $s$  is the sample thickness,  $\omega_0$  is the applied microwave frequency, and  $M$  is the saturation magnetization of the sample. This equation is derived with the boundary condition that the amplitude goes to zero at infinity. If we introduce a metal film, the equation for the velocity becomes<sup>7,8</sup>

$$V(k) = \frac{\gamma^2 s \pi M}{\omega_0} \left[ 4\pi M (e^{-2|k|t} + 1) \right] - 2N\gamma\pi s M e^{-2|k|t} \quad (2)$$

<sup>a</sup>jonathantrossman2014@u.northwestern.edu

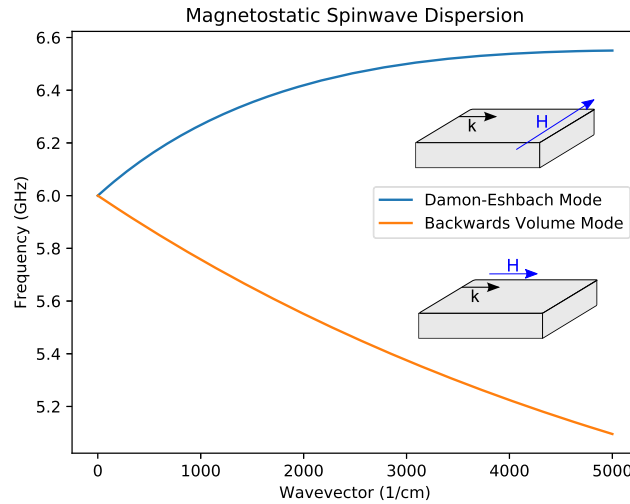


FIG. 1. Dispersion relations for the Damon-Eshbach and backwards volume modes for a YIG film with thickness  $3.05 \mu\text{m}$  in a field of 1.4 kG.

where  $N = k/|k|$ , and  $t$  is the separation of the conducting surface from that of the ferromagnet. The direction of  $k$  in the definition of  $N$  depends on the field direction such that  $N = -1$  for propagation on the side nearest the metal surface and  $N = 1$  for the side furthest.

## II. APPARATUS

Figure 2 shows a block diagram of the experiment. The YIG sample used here was supplied by MDI Corporation: it is  $5\text{mm} \times 10\text{mm}$  with a stated thickness of  $3.05 \mu\text{m}$  and was grown epitaxially on a gadolinium gallium garnet (GGG) substrate. The copper ground plane was provided by a square section of printed circuit board which forms an integral part of the sample probe and against which

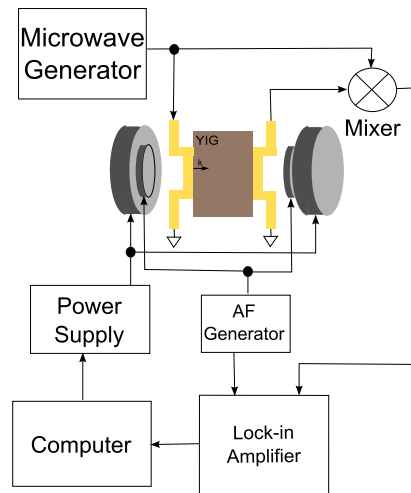


FIG. 2. Block diagram of the apparatus used. Microwaves are applied to an antenna on one side of a YIG sample. Depending on the field applied and the frequency of the microwaves, a spin wave with a particular wavevector will be launched across the sample. This spin wave is then picked up by a second antenna on the opposite side of the sample. A portion of the input signal and the output of the second antenna are then combined in a mixer, the output of which depends on the phase difference between the source and the received spin wave. As we vary the field, the wavevector of the spin wave will vary along with the output of the mixer. A small modulation field is applied to allow for lock-in detection of the mixed signal.

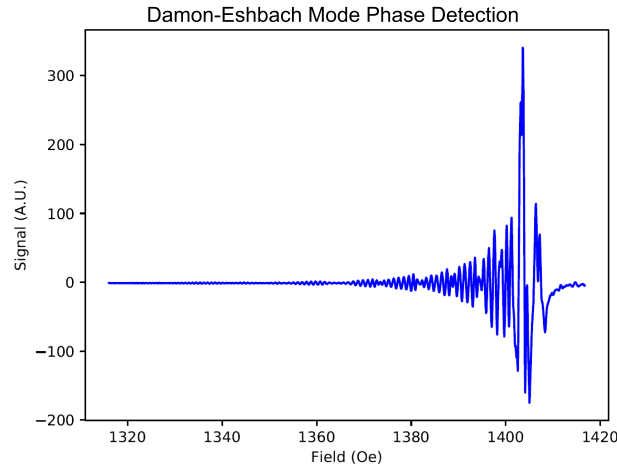


FIG. 3. A measurement of propagation in the Damon-Eshbach mode for the sample on a dielectric.

the sample was pressed. Transmitting and receiving antennas separated by 5mm were positioned on opposing sides of the sample. Each consisted of a wire running from a grounded SMA connector along the 10mm length of the sample which was grounded on the far side. (An alternate antenna design, which will not be described here, was used for metal free propagation experiments).

6 GHz microwaves are applied to one of the antennas. When the conditions defined by the Kittel equation together with the dispersion relation are met for a given magnetic field, spin waves of the corresponding wavevector will be launched perpendicular to the transmitting edge and propagate to the receiving antenna on the other side of the sample. As we vary the field, the wavevector of the spin wave will also vary. If we apply a portion of the input microwave signal and the receiver antenna output to opposite ports of a microwave mixer, the resulting signal will be controlled by the phase difference. This phase difference,  $\Delta\phi$ , is related to the change in wavevector,  $\Delta kd = \Delta\phi$ , where  $\Delta k$  is the change in wavevector for a change in field,  $\Delta H$ , and  $d$  is the width of the sample.

The detected signal for the Damon-Eshbach geometry and in the absence of a metallic boundary is shown in figure 3. The change in wavevector results in an oscillatory signal output from the mixer. Additionally, coupling to the exchange split backwards volume modes where they intersect the Damon-Eshbach mode results in nodes.<sup>9,10</sup> The spin wave velocity can be calculated using the oscillation period since a full period involves a change in phase of  $2\pi$ , which corresponds to a change in wavevector of  $\Delta k = \frac{2\pi}{d}$ . When combined with the large path length (5 mm), this allows us to make measurements of the velocity with high resolution in  $k$ , which is, in turn, made possible by the low damping in YIG.

### III. RESULTS

Figure 4 shows the field dependence of the output of the phase detector for the DE geometry for four different field/wavevector configurations in which a copper layer is in contact with the free side of the YIG film. The upper left panel shows the data for a nominally positive field and positive wavevector. The upper right panel shows the result of reversing the magnetic field direction while the lower left figure is the result of reversing the wavevector direction (simply by reversing which antenna we apply the microwave signal to). The propagation of the spin waves is clearly different between the first case and the second two cases. Instead of fast oscillations with periodic nodes due to the exchange split backwards volume modes, we observe a slow oscillation. Finally, in the lower right of figure 4 we show the data when both the field direction and the wavevector are reversed and we completely recover our original signal.

The large change in oscillation period arises from the differing characteristics of the DE mode when the wave is concentrated at the dielectric and metal interfaces. Given that the coupling to the DE mode is maximally when the magnetic field is perpendicular to the wavevector, there are two

## Signal Vs. Field With Phase Detection

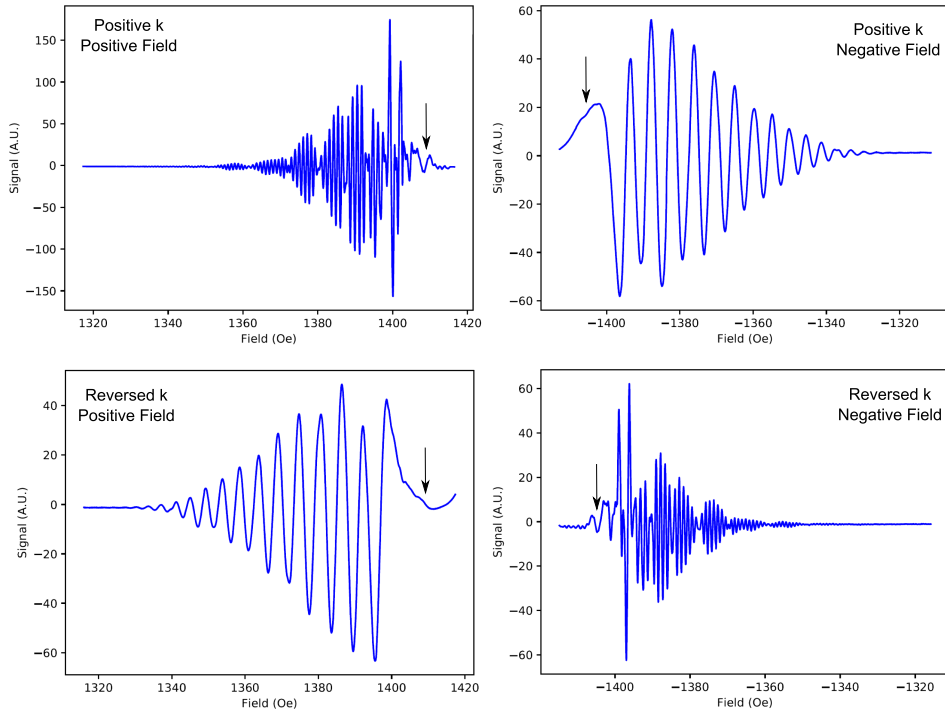


FIG. 4. Examples of data taken for a YIG film pressed against a copper ground plane for various combinations of field and wavevector direction with the upper left being the reference figure. Arrows point to the position of the ferromagnetic resonance (FMR). The figures on the right show the result of reversing the magnetic field direction while the bottom figures show the result of reversing the direction of propagation. Clear nonreciprocity of the spin waves is shown, where the upper right and lower left correspond to a wave concentrated on the YIG/copper interface. The upper left and lower right correspond to a wave concentrated on the YIG/GGG interface. Small asymmetries in the measured field are observed in between the positive and negative field measurements.

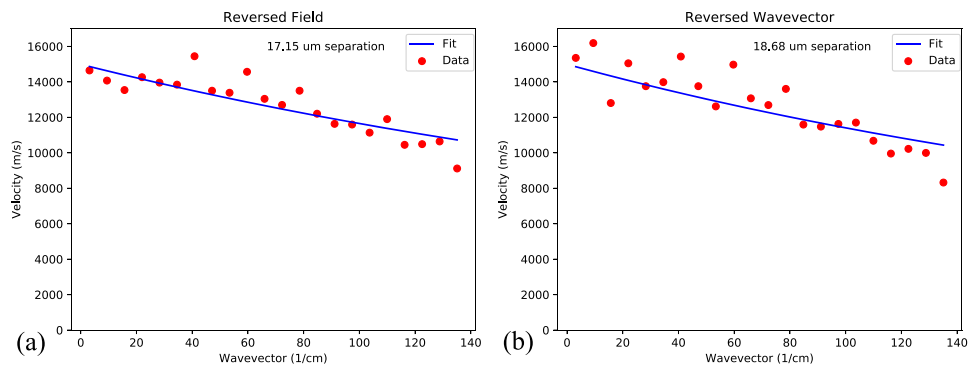


FIG. 5. The upper right and lower left of figure 4 can be used to calculate the change in wavevector with field by noting that each full period of oscillation is a change in spin wave phase of  $2\pi$  and corresponds to a change in wavevector of  $2\pi/d$ , where  $d$  is the width of the sample. This change in wavevector for a change in field can be converted to velocity using equation 1. This velocity vs. wavevector data can be fit using equation 2 to determine both the separation of the metal to the YIG and the absolute value of the wavevector. The change in velocity as  $k$  increases seems to be captured well by equation 2. The distance between the YIG sample and the metal film are determined to be  $17.15 \pm 2.82 \mu\text{m}$  and  $18.68 \pm 3.98 \mu\text{m}$  for the forward and reversed propagating waves respectively. (a) Velocity versus field for positive field with a fit from equation 2 where the spin wave is nearest the metal film. Corresponds to the lower left plot of figure 4. (b) Velocity versus field for negative field with a fit from equation 2 where the spin wave is nearest the metal film. Corresponds to the upper right plot of figure 4.

possible configurations, each corresponding to the wave traveling on opposing surfaces of the sample. The upper left and lower right figures corresponds to a wave concentrated on the YIG/GGG interface while the upper right and lower left figures correspond to a wave concentrated at the YIG/Copper interface.<sup>11</sup> Clearly the effect of the metal film is largest in the latter configuration.

From figure 4 we can determine the change in wavevector with field. To convert this to a change in wavevector with frequency we use the Kittel equation,  $\omega_0 = \gamma\sqrt{H(H + 4\pi M)}$ , and the relation

$$V = \frac{d\omega}{dk} = \frac{dH}{dk} \frac{d\omega}{dH} \quad (3)$$

We can then fit the velocity as a function of wavevector using equation 2 for the separation of the metal as shown in figure 5. Here we find  $17.15 \pm 2.82 \mu\text{m}$  and  $18.68 \pm 3.98 \mu\text{m}$ . A more complete interpretation of our data will require the inclusion of the effects of a finite conductivity in the adjacent metal.<sup>2</sup> The thicknesses obtained here then models this effect, the actual gap then being smaller than the fitted gap.

#### IV. CONCLUSION

In this paper we have demonstrated the effect of a metal surface on Damon-Eshbach mode spin waves, which is in accordance with equation 2. Using this equation, one can extract (effective) values for the separation between the metal surface and the ferromagnetic sample.

#### ACKNOWLEDGMENTS

This research was carried out under support from the U.S. Department of Energy through grant DE-SC0014424.

- <sup>1</sup> A. A. Stashkevich, M. Belmeguenai, Y. Roussigné, S. M. Cherif, M. Kostylev, M. Gabor, D. Lacour, C. Tiusan, and M. Hehn, "Experimental study of spin-wave dispersion in py/pt film structures in the presence of an interface Dzyaloshinskii-Moriya interaction," *Physical Review B* **91**(21), 214409 (2015).
- <sup>2</sup> M. Mruczkiewicz and M. Krawczyk, "Nonreciprocal dispersion of spin waves in ferromagnetic thin films covered with a finite-conductivity metal," *Journal of Applied Physics* **115**(11), 113909 (2014).
- <sup>3</sup> R. W. Damon and J. R. Eshbach, "Magnetostatic modes of a ferromagnet slab," *Journal of Physics and Chemistry of Solids* **19**(3-4), 308–320 (1961).
- <sup>4</sup> W. L. Bongianni, "Magnetostatic propagation in a dielectric layered structure," *Journal of Applied Physics* **43**(6), 2541–2548 (1972).
- <sup>5</sup> A. Kreisel, F. Sauli, L. Bartosch, and P. Kopietz, "Microscopic spin-wave theory for yttrium-iron garnet films," *The European Physical Journal B-Condensed Matter and Complex Systems* **71**(1), 59–68 (2009).
- <sup>6</sup> B. A. Kalinikos and A. N. Slavin, "Theory of dipole-exchange spin wave spectrum for ferromagnetic films with mixed exchange boundary conditions," *Journal of Physics C: Solid State Physics* **19**(35), 7013 (1986).
- <sup>7</sup> D. D. Stancil and A. Prabhakar, *Spin waves* (Springer, 2009).
- <sup>8</sup> S. R. Seshadri, "Surface magnetostatic modes of a ferrite slab," *Proceedings of the IEEE* **58**(3), 506–507 (1970).
- <sup>9</sup> W. Schilz, "Experimental evidence for coupling between dipole and exchange dominated spin waves in epitaxial yig," *Solid State Communications* **11**(5), 615–616 (1972).
- <sup>10</sup> J. D. Adam, T. W. O'Keeffe, and R. W. Patterson, "Magnetostatic wave to exchange resonance coupling," *Journal of Applied Physics* **50**(B3), 2446–2448 (1979).
- <sup>11</sup> R. E. Camley, "Nonreciprocal surface waves," *Surface Science Reports* **7**(3-4), 103–187 (1987).